Modeling Conformal Array Antennas of Various Shapes Using Uniform Theory of Diffraction (UTD)

(Invited paper)

Patrik Persson
Royal Institute of Technology, Division of Electromagnetic Engineering,
SE-100 44 Stockholm, Sweden; E-mail: patrik.persson@ee.kth.se

Abstract - Traditionally, antennas have been designed as separate components, mounted on e.g. masts, buildings, and vehicles. Modern systems, however, require antennas to be integrated with existing structures. This paper discusses the analysis of conformally integrated array antennas using the hybrid UTD-MoM method, in particular arrays on doubly curved surfaces. Computed results are shown including singly and doubly curved surfaces. Most of the results are verified by measured results and calculated results obtained with a modal solution.

I. INTRODUCTION

The rapid growth in wireless communications, especially mobile communications, has caused the requirements on antenna systems to be more and more demanding. For future antenna systems a typical requirement is to integrate the antennas in the surface of different vehicles or platforms. For example, a modern aircraft has today many antennas protruding from the structure, for navigation, various communication systems, instrument landing systems, radar altimeter and so on. Integrating these antennas into the aircraft skin is highly desirable [1]. Antennas can also be integrated in various structures such as lampposts, chimneys, even trees, etcetera, in order to be more easily accepted by the public, as shown in Figure 1.

The need for such antennas, *conformal antennas*, is even more pronounced for the large apertures that are necessary in *e.g.* satellite communication and military airborne surveillance radars. In order to ensure proper operation of these systems, it is important to be able to determine the characteristics of the antennas. Thus, efficient (numerical) methods suitable for the analysis of conformal antennas are needed.

This paper will discuss modeling of conformal array antennas, in particular, antennas on electrically large, doubly curved surfaces. The emphasis is on the numerical implementation. The results are verified with measured data, but also with a modal solution. The layout of the paper is as follows; first, methods of analysis are discussed in general, but the main focus will be on the hybrid UTD-MoM method. This includes a discussion about geodesic ray tracing on surfaces with varying curvature. Finally, results are given to illustrate the accuracy of the hybrid method for singly and doubly curved PEC surfaces. The antenna element used through out this paper is the waveguide-fed aperture antenna, both with rectangular and circular cross-sections.

Figure 1. Possible location for base station antennas [2].

II. METHODS OF ANALYSIS

Important steps in the analysis of conformal array antennas are to find the mutual coupling among the radiating elements and the (isolated and/or embedded) radiation patterns of the individual elements. A critical step in the analysis is therefore to find the electromagnetic fields on the surface and in the far-field in the presence of a complex and arbitrarily shaped body. This is, in general, a difficult problem since the surface is often large (in terms of wavelength) and it may be convex or concave or both. Furthermore, the surface can have edges and other discontinuities, and a dielectric layer can cover the antenna aperture.

The available methods are often divided into two categories; frequency domain methods and time domain methods. Frequency domain methods are probably the most commonly used methods for analysis of antennas, including conformal antennas. Thus, our focus will be on these methods -- the interested reader can find an overview of time domain methods (mainly FDTD and techniques to avoid staircase approximation errors) in [3].

The classical way of analyzing conformal antennas is to use a modal solution. Such a solution is possible to obtain only for some special cases like a perfectly conducting circular cylinder, elliptic cylinder, cone, or sphere [4]. However, if the geometry is more complex, *e.g.* a rotationally symmetric surface of arbitrary cross section, a modal solution is very difficult, if at all possible, to obtain. The analysis is also typically highly complex and suffers convergence problems when the size of the geometry is increased (in terms of wavelengths). Hence, the process of extracting numerical results can be difficult and very time-consuming. A simplification of the modal solution for structures with rotational symmetry is to reduce the 3D problem to a spectrum of 2D problems by applying a Fourier transformation with respect to the symmetry axis as described by R. F. Harrington [5].

For arbitrarily shaped (3-D) bodies no exact analytical solutions exist. In the low frequency range, several reliable numerical procedures, *e.g.* method of moments (MoM) [6] and the finite element methods (FEM) [7], are available for solving the radiation/scattering problem. However, for higher frequencies, these numerical techniques become impractical since the associated matrix becomes very large.

One way of avoiding these problems is to use a high frequency approach. The term high frequency means that the fields are being considered in a system where the properties and size parameters of the geometry vary slowly with the frequency. This is not a serious limitation in many cases since the minimum radius of curvature of the surface can be quite small. A commonly used requirement is $kR \geq 2-5$ (k is the wave number, R is the radius of the cylinder) for accurate results [8]. From an engineering point of view these conditions are often fulfilled for large bodies when the frequency is in the microwave frequency band or higher.

There are a number of different high frequency techniques, or asymptotic techniques, available. The reason is that an asymptotic technique is often specialized for a certain problem and cannot be generalized easily. However, a general formulation is very desirable for efficient analysis of various realistic conformal antennas. A well known formulation is the ray-based uniform theory of diffraction (UTD) [9-11]. This approach has been successful and the solution is useful for different types of convex PEC surfaces, including doubly curved surfaces. Note, however, that UTD also has disadvantages as will be discussed later.

If coated surfaces are considered there is no general tool for electrically large surfaces. For the special case of circular cylinders an efficient high frequency method is described in [12-13], valid in the non-paraxial region. For coated circular cylinders and spheres of moderate sizes, an efficient modal solution is described in [14].

An overview of different frequency domain methods suitable for conformal antennas, including a comparison of different methods, can be found in [3].

III. THE HYBRID UTD-MOM APPROACH

As indicated in the previous section all methods have their advantages and disadvantages. To overcome the disadvantages a hybrid approach (a combination of different methods) is often used in practice. A commonly used method when analyzing conformal antennas is the hybrid UTD-MoM method, an alternative is the FE-BI method [15]. In the following, we will discuss the UTD-MoM method applied to waveguide-fed aperture antenna arrays on curved PEC surfaces. We will first present the general approach and then some aspects of the UTD formulation. Finally, the issue of finding ray paths (geodesics) on curved surfaces is described.

A. General formulation

The approach is based on the integral equation formulation, solved by the MoM. As will become clear, the general analysis is not any different from the planar case. However, it is more difficult to find the field representation outside a curved surface.

Figure 2 shows the waveguide-fed aperture problem for aperture m with the computational domain divided into two regions, the interior and exterior regions. By using the field equivalence theorem [5, page 106] an equivalent (exterior) problem is obtained by covering the apertures with a perfectly conducting surface and introducing unknown equivalent magnetic current moments on the surface. These infinitesimal magnetic current moments then radiate in the presence of the curved perfectly conducting surface.

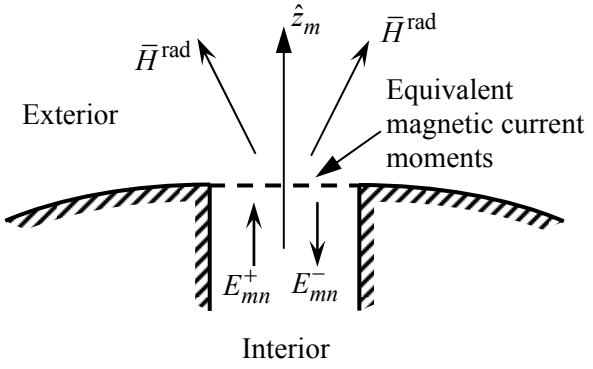

Figure 2. The interior and exterior domains at aperture m with the n^{th} waveguide mode for a PEC surface.

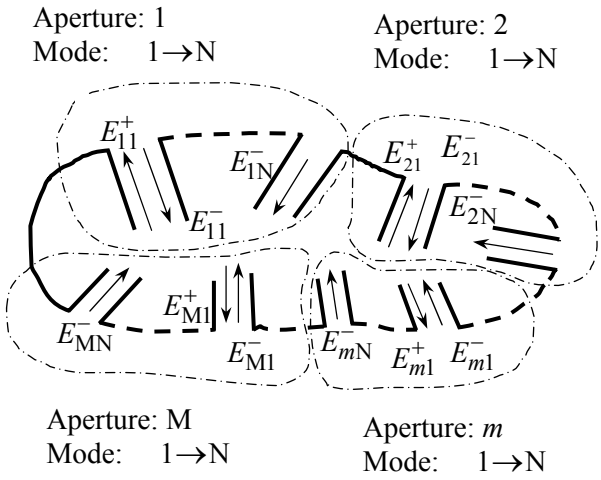

Figure 3. A symbolic picture of the physical and electrical ports in the antenna array.

Applying the boundary condition for the tangential magnetic field results in the following integral equation;

$$\bar{H}^{\text{ext}}_{\tan}\Big|_{\bar{r}\in S^+_{ap}} = \bar{H}^{\text{int}}_{\tan}\Big|_{\bar{r}\in S^-_{ap}} \tag{1}$$

where S_{ap} is the set of all apertures, $\bar{H}^{\text{ext}}_{\tan}$ is the external surface field caused by the equivalent magnetic current moments, and $\bar{H}^{\text{int}}_{\tan}$ is the magnetic field in the interior region.

Let us now consider an array with M apertures and N modes in each aperture. The antenna array can be treated as a $\text{M}\times\text{N}$ port circuit according to Figure 3. Hence, the aperture magnetic field in the internal region is given as

$$\bar{H}^{\text{int}}_{\tan}\Big|_{\bar{r}\in S^-_{ap}} \approx \sum_{m=1}^{M}\sum_{n=1}^{N}\left[Y^n_g E^+_{mn}\left(\hat{z}_m\times\bar{e}^n_m\right) - Y^n_g E^-_{mn}\left(\hat{z}_m\times\bar{e}^n_m\right)\right]. \tag{2}$$

Equation (2) expresses the field expanded into a series of basis functions. Here, we have used the waveguide modes $\left(\bar{e}^n_m\right)$ in the waveguide as basis functions with unknown amplitudes E^+_{mn} and E^-_{mn} (Y^n_g is the modal admittance). The plus sign indicates a wave propagating towards the aperture and the minus sign a wave propagating away from the aperture Note that we have used a single mode index n to represent the triple mode index i, j, TE/TM where i, j are the usual mode indices and TE/TM is an index that indicate TE- or TM-mode.

It should be noted that throughout this paper the transmitting apertures are fed by the dominant waveguide mode only. However, at the different waveguide openings, see Figure 2, infinitely many reflected evanescent modes are generated. Also at the receiving apertures infinitely many modes are generated from the external field. A single/dominant mode approximation is often used, but for a more accurate analysis higher order modes are needed as will be discussed later.

To solve for the unknown modal amplitudes, (2) is inserted into (1). The discretized integral equation is then transferred to a matrix equation by using Galerkin's method (*i.e.* weighting functions = basis functions) with the inner product defined as $\left\langle \bar{f},\bar{g}\right\rangle = \iint\left(\bar{f}\cdot\bar{g}\right)dS$. We get

$$\sum_{m=1}^{M}\sum_{n=1}^{N}\left[E^+_{mn}\underbrace{\left\langle \bar{H}^{\text{ext}}_{\tan}\left(\bar{e}^n_m\right),\hat{z}_p\times\bar{e}^q_p\right\rangle}_{Y^{qn}_{pm}} + E^-_{mn}\underbrace{\left\langle \bar{H}^{\text{ext}}_{\tan}\left(\bar{e}^n_m\right),\hat{z}_p\times\bar{e}^q_p\right\rangle}_{Y^{qn}_{pm}}\right]\Bigg|_{\bar{r}\in S^+_{ap}} =$$

$$\sum_{m=1}^{M}\sum_{n=1}^{N}\left[Y^n_g E^+_{mn}\underbrace{\left\langle \hat{z}_m\times\bar{e}^n_m,\hat{z}_p\times\bar{e}^q_p\right\rangle}_{\delta^{qn}_{pm}} - Y^n_g E^-_{mn}\underbrace{\left\langle \hat{z}_m\times\bar{e}^n_m,\hat{z}_p\times\bar{e}^q_p\right\rangle}_{\delta^{qn}_{pm}}\right] \forall p,q \tag{3}$$

As seen, the mutual admittance $\left(Y^{qn}_{pm}\right)$ between modes $n\to q$ in the apertures $m\to p$ is directly identified in

equation (3). Hence, both the mutual admittance and the unknown modal amplitudes $\left(E_{mn}^{+}, E_{mn}^{-}\right)$ can be found if $\bar{H}_{\tan}^{\text{ext}}\left(\bar{e}_m^n\right)$ is known. From the modal amplitudes the far-field radiation pattern can be calculated.

A very important parameter in the analysis of (conformal) array antennas is the mutual coupling among the elements. Of interest is the scattering matrix which can be found easily since the mutual admittances are directly identified in (3). The scattering matrix is given by the following formula

$$\mathbf{S} = \left(\mathbf{I} - \mathbf{Y}\right)\left(\mathbf{I} + \mathbf{Y}\right)^{-1}. \tag{4}$$

Note that two cases can be distinguished. The first is the mutual coupling between two elements only, referred to as the isolated coupling since no other elements are involved. The other elements of the array are assumed to be absent (short circuited in case of apertures). For this case, $\mathbf{Y}$ is a 2×2 element matrix calculated as a function of the spacing or any other parameter of interest. With all elements present we use the term array mutual coupling. The array mutual coupling is obtained by considering all elements in the array, thus $\mathbf{Y}$ is an $\mathrm{M}\times\mathrm{M}$ element matrix where M is the number of elements in the array. If higher order waveguide modes are used in the analysis the matrix is of the size $\mathrm{MN}\times\mathrm{MN}$ where N is the number of modes used (see equation (3)).

An important observation is that the integral equation is referred to the curved aperture plane. However, the basis functions $\left(\bar{e}_m^n\right)$ are valid in a planar surface in a cross section of the waveguide. See Figure 4 where the planar surface in the waveguide is shadowed. Despite this fact, the fields at the convex surface are often assumed to be the same as in the waveguide and the gap in Figure 4 is disregarded.

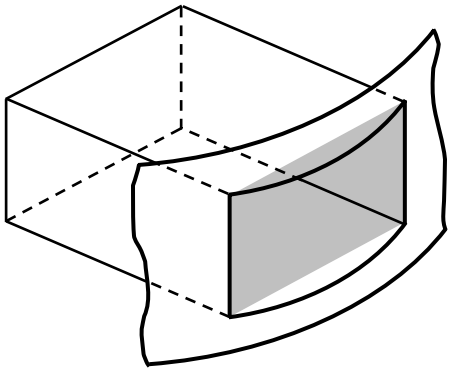

Figure 4. The geometry at the aperture.

In many applications this approximation may be tolerable, especially if the radius of curvature is large in the "wide" plane of the aperture. But, if the radius of curvature becomes smaller, the error may become too large. One way of reducing the error is to add a phase to the aperture field at the planar surface to include the small distance to the curved surface. This is done in the simulations presented in this paper.

B. The Uniform Theory of Diffraction (UTD)

The uniform theory of diffraction was developed to retain all the advantages of GTD and overcome the failure of GTD in the shadow boundary transition region. Assuming that the principal radius of curvature of the surface is large in terms of wavelength, and slowly varying along the surface, it was possible to obtain uniform asymptotic solutions to the canonical problems of diffraction by perfectly conducting circular cylinders and spheres [9-11]. These solutions can then be generalized to arbitrary convex surfaces with the aid of the local properties of high frequency wave propagation.

In this section, we limit the discussion to the surface field only, since it is needed in order to solve the integral equation for the unknown modal amplitudes (and the mutual coupling)[#]. The formulas will, however, not be repeated here, and the reader is referred to the papers indicated above for all details. The focus will be on a couple of complications that exist in the UTD solution.

It is well known that the UTD solution experiences problems when the ray path approaches the axial direction of the cylindrical geometry. The reason is that the approximation used for the fields in terms of Fock type Airy functions cannot be completely justified in the paraxial region. However, limiting forms for the components of the surface dyadic Green's function can be obtained for the PEC surface. This approach seems to give results accurate enough, and is used throughout this paper. But there is also an alternative, more accurate, solution available for the paraxial region. It is obtained by including higher order terms in the asymptotic evaluation of the exact solution and was presented by Boersma and Lee [16].

Another disadvantage with UTD is that small details cannot be included. Due to the approximations used in the derivation, the distance between the source and field points must be larger than circa 0.5λ. This is a problem, especially when calculating the self admittance since the dyadic for the surface magnetic

[#] The radiation pattern can be found using the formulas in [10] once the modal amplitudes are found.

field has a s^{-3} singularity as $s \to 0$ (s is the distance between the source and field points). For the circular cylinder Yung et al. [17] has shown that it is possible to rewrite the dyadic for the surface magnetic field with the help of the planar Green's function. Thus, a regularization can be obtained if the surface dyadic Green's function $\bar{\bar{G}}$ is rewritten as

$$\bar{\bar{G}} = \bar{\bar{G}}^{\text{pl.}} + \underbrace{\bar{\bar{G}}^{\text{cyl.}}_{\text{asympt.}} - \bar{\bar{G}}^{\text{pl.}}_{\text{asympt.}}}_{\bar{\bar{G}}^{\text{pert.}}} \tag{5}$$

The second term in (5) can be viewed as a perturbation due to the curvature of the circular cylinder. Furthermore, note that the asymptotic cylindrical dyadic is still used in (5). This is possible, at least when calculating the self admittance of the dominant TE_{10} mode as shown in [18]. The only requirement is that the cylinder radius exceeds about two wavelengths. This requirement is often fulfilled in most practical applications. An explicit expression for the self admittance of the dominant TE_{10} mode, based on the above approach, is found in [19]. The outlined approach can also be used for arbitrarily shaped singly curved surfaces by approximating the surface at the aperture location with a circular cylinder. The radius of the circular cylinder then equals the local radius of curvature at the element position.

Another possible approximation for handling small separations between source and field points is to use a planar solution.. Comparison of the planar approach and the above mentioned regularization process has shown that the planar approximation gives satisfactory results for the geometries of practical interest. A rigorous study for doubly curved surfaces has, to the author's knowledge, not been performed. But, it can be assumed that the planar approximation is accurate enough for most applications. Hence, in the calculations made in this paper the planar approximation is used both for singly and doubly curved surfaces. The result is satisfactory as will be seen later.

C. Geodesics

Before UTD can be applied to curved surfaces it is important to find the proper ray(s) that connect(s) arbitrarily located points on a smooth surface. For a correct solution, the rays must obey certain conditions in order to be valid geodesics on the surface. A complete treatment of this problem is beyond the scope of this paper, the interested reader is referred to textbooks on differential geometry (see e.g. [20]), but some highlights will be discussed with emphasis on doubly curved surfaces.

In its most general form, the geodesics are given by a second order differential equation, which satisfies the generalized Fermat's principle. Unfortunately, the solution to the differential equation is often difficult to find explicitly; instead some kind of numerical (ray tracing) procedure has to be used. Anyhow, every solution (it may be more than one!) that fulfills the geodesic equation is called a geodesic, whether it is an arc of shortest distance or not. Thus, geodesics may be regarded as *stationary* curves rather than strictly shortest distances on the surface. Hence, a general definition of a geodesic is that "along the geodesic the principal normal ($\hat{n}$) coincides with the surface normal ($\hat{N}$)". Figure 5 illustrates a situation when a curve along the surface is not a geodesic.

Fortunately, the ray tracing procedure can be simplified for certain geometries. This considerably reduces the numerical computations. The class of surfaces that can be analyzed in this way belongs to the geodesic coordinate system (GCS) [20], *i.e.* the parameter lines of the surface are orthogonal to each other. In these cases the geodesic equation is reduced to a first order differential equation. Examples of surfaces that belong to the GCS are any of the eleven surfaces defined by the Eisenhart coordinate system. Actually, the analysis presented here can also be extended to non-Eisenhart surfaces. The only requirement is that the surface can be defined in the GCS. One example of a non-Eisenhart surface is the ogive, which is of great interest in aerospace engineering since it can describe many of the shapes encountered in the area. The ogive is not a coordinate surface of an Eisenhart coordinate system but can be identified as the coordinate surface of the bispherical coordinate system [21], which fulfills the requirements. Thus, a straight forward analysis can be performed for many geometries of interest within the conformal antenna area.

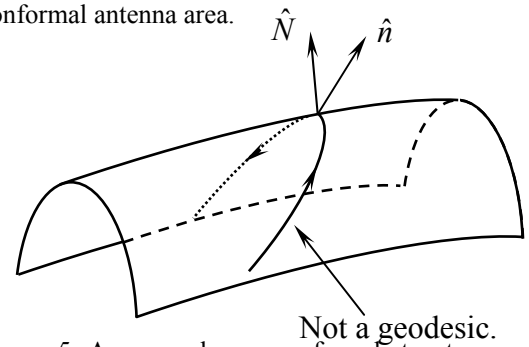

Figure 5. A curve along a surface, but not a geodesic surface ray.

Assume that the parametric equation of the surface is $x_i = X_i(u,v),\ i = 1...3$ where u and v are the curvilinear coordinates, within a certain closed interval.

Then, the geodesic equation for the surfaces belonging to the GCS is given as

$$v(u)=\underbrace{\int \frac{\pm\alpha\sqrt{E}}{\sqrt{G}\sqrt{G-\alpha^2}}du}_{\Im(u,\alpha)}+\beta \tag{6}$$

where E and G are two out of three so called first fundamental coefficients [20]. α is a constant of integration, known as the first geodesic constant. The $\pm$ sign in front of α depends on whether v is monotonically increasing or decreasing with u. β is the second geodesic constant. The physical significance of α and β is that they uniquely characterize a geodesic.

The solution to (6) provides the general solution for the specific geometry. To find the particular solution that connects two points on a surface the geodesic constants α and β have to be found. Since the positions of the different antenna elements are known, as well as the field or diffraction points, α and β can be found by solving the following system of equations

$$\begin{aligned} v_{\text{start}} &= \Im(u_{\text{start}},\alpha)+\beta, \\ v_{\text{stop}} &= \Im(u_{\text{stop}},\alpha)+\beta. \end{aligned} \tag{7}$$

The analysis is facilitated since the integral in (6) can be solved in closed form for the surfaces defined by the Eisenhart coordinate system! Furthermore, both the ray parameters of the differential type as well as the integral type in the UTD formulation can be found directly for the geometries discussed here with the aid of differential geometry. In fact, the only unknown in these expressions is the first geodesic constant α. Hence, the accuracy of the results obtained with UTD depends exclusively on the accuracy of the first geodesic constant α. As a consequence some authors have called the method the geodesic constant method (GCM) [22].

Analyzing singly curved surfaces is straightforward since they are developable surfaces. Thus, they can be unfolded and analyzed as flat surfaces and the key parameters in the UTD formulation are obtained from a two-dimensional analysis. Hence, they can be studied directly without solving the geodesic equation.

More interesting is the solution of the geodesic equation for doubly curved surfaces. Any rotational symmetric, doubly curved surface can be described, in parametric form, as

$$x=f(u)\cos v,\ y=f(u)\sin v,\ z=g(u) \tag{8}$$

and the solution to the geodesic equation (6) becomes

$$v(u)=\int \frac{\pm\alpha\sqrt{\left(f'(u)\right)^2+\left(g'(u)\right)^2}}{f(u)\sqrt{\left(f(u)\right)^2-\alpha^2}}du+\beta\,. \tag{9}$$

For the case of a sphere $\left(x=a\sin\theta\cos\varphi,\ y=a\sin\theta\sin\varphi,\ z=a\cos\theta\right)$ the geodesics are given by:

$$\varphi=-\tan^{-1}\left[\frac{\alpha\cos\theta}{\sqrt{a^2\sin^2\theta-\alpha^2}}\right]+\beta\,. \tag{10}$$

The paraboloid of revolution $\left(x=au\cos\varphi,\ y=au\sin\varphi,\ z=-u^2\right)$ has the following solution to the geodesic equation:

$$\begin{aligned} \varphi=\frac{\alpha}{a^2}\ln\frac{a\sqrt{a^2+4u^2}+2\sqrt{a^2u^2-\alpha^2}}{a\sqrt{a^2+4u^2}-2\sqrt{a^2u^2-\alpha^2}}+ \\ \sin^{-1}\left[\frac{a\sqrt{a^2u^2-\alpha^2}}{u\sqrt{a^4+4\alpha^2}}\right]+\beta. \end{aligned} \tag{11}$$

Additional explicit formulas for geodesics on singly and doubly curved surfaces are found in [3].

One important factor, as already indicated, is that the accuracy of the field solution depends on the accuracy of α. It has been stated that α must be computed accurately with up to eight decimal places for a given arbitrary set of source and observation points [23]. By changing the value of α from the correct result the angular distance will change resulting in a shorter or longer geodesic. In the analysis of conformal antennas some surface-ray parameters will then change and in the worst case give unsatisfactory results. To keep the angular distance within one tenth of a degree (assuming the field and observation points are at the same z-value of a paraboloid) α has to be computed accurately up to four decimal places for this example. If eight decimals are correct the angular difference will change no more than about 0.000005^{o} in this case. Another example is shown in Figure 6 where a paraboloid is considered with: $a=1.0$, $u_{\text{start}}=0.5$, $u_{\text{stop}}=2.5$ and $\left|\varphi_{\text{stop}}-\varphi_{\text{start}}\right|=130^{\text{o}}$. In this example the correct geodesic is shown together with two geodesics when

the correct value of α is increased and decreased, respectively, with 1%. The result is an angular difference of circa 3 degrees. Hence, as shown here, it is probably not necessary to compute α with up to eight decimal places in the practical analysis of conformal antennas.

Another important factor when analyzing doubly curved surfaces is the geodesic splitting phenomenon. It appears for certain combinations of source and observation coordinates for which the geodesic equation can result in two distinct values for α, thereby resulting in two distinct geodesics for a given direction and order. This may be surprising since it is well known that between any two arbitrarily located points on a cone or a cylinder, there exists primary and higher-order (of multiple encirclements) geodesics in both anticlockwise and clockwise directions. However, the number of geodesics of a given order and direction never exceeds one. In contrast, for doubly curved surfaces the geodesic of a given order and direction can be split into two! For the paraboloid this phenomenon appears when the start and stop positions have the same z-value, but with an angular distance $\geq 180^{\mathrm{o}}$. Figure 7 shows an example of the splitting phenomena for a paraboloid with $a = 1.6$, $u_{\mathrm{start}} = u_{\mathrm{stop}} = 2$, and $\left|\varphi_{\mathrm{stop}} - \varphi_{\mathrm{start}}\right| = 220^{\mathrm{o}}$.

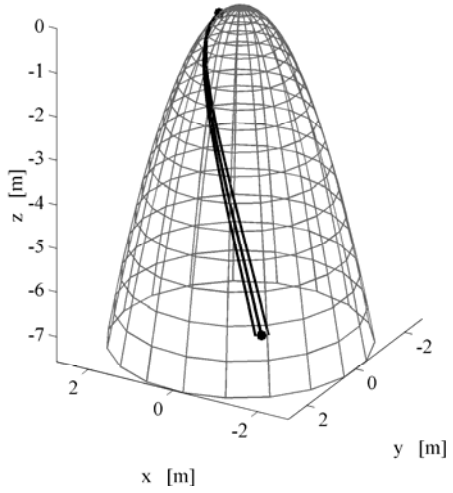

Figure 6. One example where the angular difference has changed with 3 degrees when α was changed ±1%.

Unfortunately, there is no a priori method of identifying which geodesics are the dominant contributors to the total surface ray field. Thus, the splitting phenomenon gives, in general, an unavoidable doubling of the computations. However, in most cases the arc length

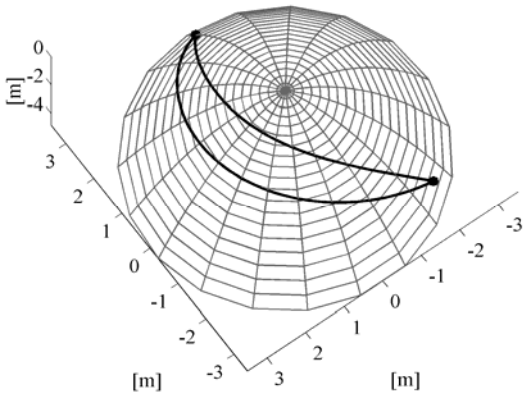

Figure 7. An example of geodesic splitting.

gives a hint about which geodesic is the dominant one since the surface ray field is decaying as a function of the arc length. Hence, the situation in Figure 7 is not critical since the geodesic traveling in the opposite direction around the surface is the shortest one. But for a more general surface there can be situations when two (or more) geodesics have about equal lengths. In such cases the arc length is no longer a useful parameter for finding the dominant surface ray path. One option is then to consider the radius of curvature since the loss of energy is also due to diffraction from the surface ray. If this does not give information enough all geodesics have to be included in the analysis.

IV. NUMERICAL RESULTS

This section discusses several examples to illustrate the accuracy and usability of the UTD-MoM method. Both singly and doubly curved PEC surfaces are considered. If a coating is present the problem becomes more difficult, especially for electrically large surfaces as discussed earlier. The results shown are in many cases verified with measured results, but the modal solution is also used to study circular cylinders with small radii.

A. Singly curved surfaces

Antennas mounted on singly curved surfaces are an important class of conformal arrays for applications where a large (azimuthal) angular coverage is required. These types of antennas have been used in many experimental radar and communication systems. An overview of different types of antennas is found in *e.g.* [3, 24].

The first example to be considered is a PEC circular cylinder with radius $R = 0.3$ m. The array consists of 54 rectangular aperture radiators with circumferential polarization. The size of the apertures is 0.016 m × 0.039 m and they are located in three rows with 18

elements in each row. Each row corresponds to an angular interval of approximately 120 degrees and the frequency is chosen to be 4.3 GHz (the cutoff frequency for the dominant TE_{10} mode is ≈ 3.8 GHz). These data correspond to an experimental antenna built by Ericsson Microwave Systems AB in Mölndal, Sweden in 1998. The antenna is shown in Figure 8.

As may be seen, the cylinder is truncated at the rear due to practical reasons. Hence, no surface rays encircling the cylinder were taken into account in the calculations (*i.e.* only a single surface ray was accounted for in the simulations). Furthermore, during the measurements, absorbers were placed on the edges to minimize edge effects. Note that the aperture in the lower left corner is aperture number 1, and aperture number 54 is located in the upper right corner.

The results shown here is the array mutual coupling, *i.e.* the coupling among the elements in the array environment with all elements present and terminated in matched loads. Additional results (other frequencies, *H*-plane coupling, radiation patterns and so on) can be found in [3, 25]. Figure 9 shows the amplitude and phase of the mutual coupling along the center row of the array, *i.e. E*-plane array coupling. In the calculations only a single waveguide mode is used.

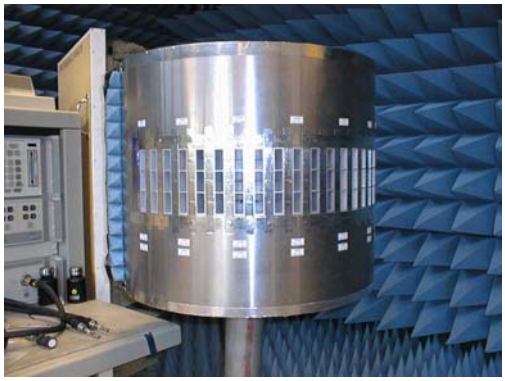

Figure 8. The experimental antenna. Courtesy of Ericsson Microwave Systems AB.

Even with a single mode approximation, the mutual coupling diagram shows good agreement between the calculated and measured results (including the self term), at least down to about -50 dB. For elements far away the agreement is not so good but here the coupling levels are very low.

In order to improve the accuracy even further, higher order waveguide modes were included in the analysis. With the four lowest TE-modes (in increasing cutoff order, *i.e.* TE_{10}, TE_{20}, TE_{01}, and TE_{11}) only small differences were observed. But when taking also the TM_{11} mode into account a significant improvement was obtained, see Figure 10. Now the simulated results show good agreement with measurements down to coupling levels as low as –80 dB. The agreement of the phase is also improved. Using even more modes (up to 20 modes were tried) improved the results very little [25]. Hence, the results are certainly sufficient for array design purposes. The importance of the TM_{11} mode is probably explained by the fact that this mode is the first mode with an electric field component parallel with the direction of propagation in the waveguide.

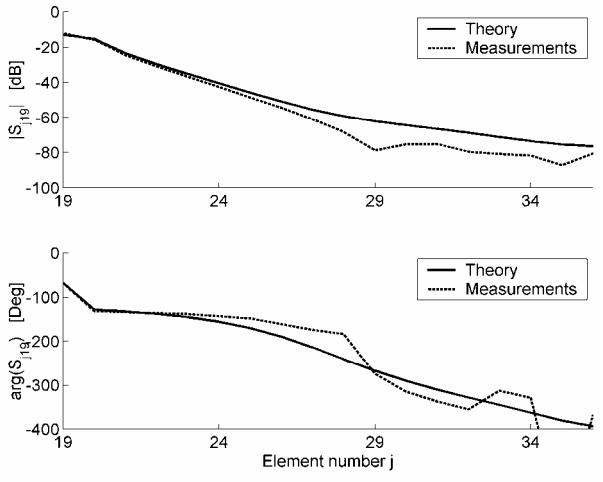

Figure 9. The array mutual coupling (including the self term $S_{19,19}$) along the center row of the array (*E* plane). Single mode approximation, $f = 4.3$ GHz.

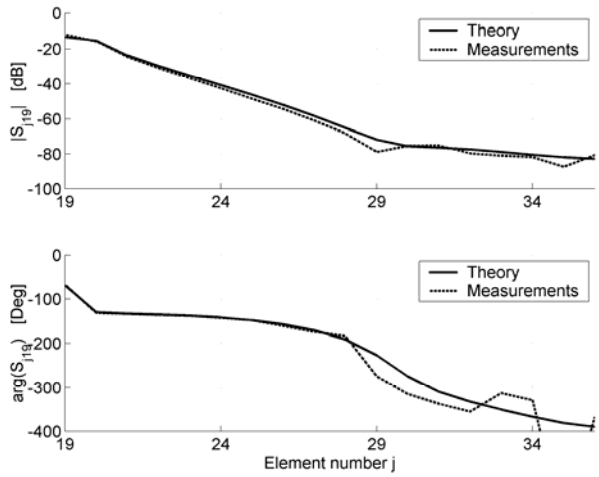

Figure 10. The array mutual coupling (including the self term $S_{19,19}$) along the center row of the array (*E* plane). 5 modes approximation, $f = 4.3$ GHz.

To investigate the ability of the UTD-MoM solution to handle electrically small surfaces, we will now consider a circular cylinder with a very small radius. The same elements as above (and frequency) is used, but the radius is reduced to 0.06 m (0.86λ). This is less than the commonly accepted limit for the UTD formulation where a radius of curvature as small as 1λ is expected to be very close to the limit. Figure 11 (a) shows the amplitude and phase of the isolated coupling between two elements as a function of the angular distance along the circumferential direction (*i.e. E*-plane coupling). Figure 11 (b) shows the case when the axial distance between the apertures is changed and equals 0.041 m (0.59λ). The angular extent in the circumferential direction is 180 degrees in both cases, and a single mode approximation is used. It has been shown [3] that the inclusion of higher order modes does not increase the accuracy in the case of isolated mutual coupling. Furthermore, two rays are included in the UTD-MoM solution – one in each direction around the circular cylinder. To be able to verify the solution a modal solution is used [4]. Generally speaking, the agreement is good and it appears as if the UTD-MoM solution recovers the canonical cylindrical solution even for small cylinders. The disagreement seen in Figure 11 (a) appears when the angular distance is less than 20 degrees. However, this equals an arc length of 0.3λ, and, as mentioned earlier, the UTD solution is supposed to be valid for distances larger than about 0.5λ.

Considered next is the PEC elliptic cylinder. By changing the ellipticity different kind of surfaces can be studied. We show the isolated mutual coupling in the *E* plane as a function of the ellipticity, *i.e.* the ratio between the major and minor axes (a/b). The

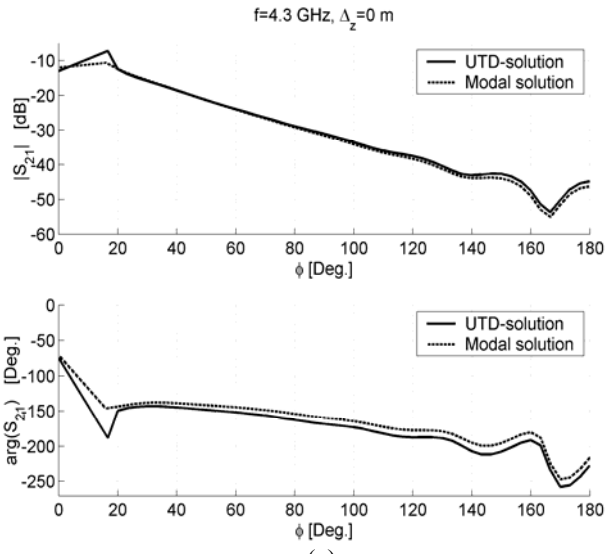

(a)

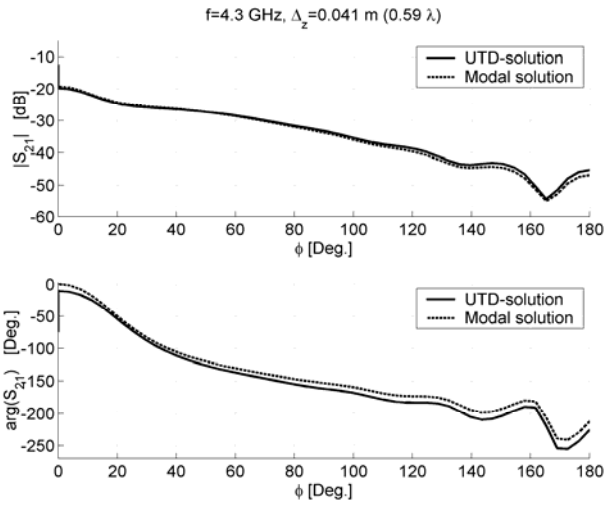

(b)

Figure 11. The isolated mutual coupling between two apertures located on a circular cylinder, $R \approx 0.86\lambda$. (a) Along the circumferential direction, *i.e. E*-plane coupling. (b) Along the circumferential direction when the two elements are 0.59λ apart in the axial direction.

transmitting element (indicated by a cross in Figure 12) is fixed, but the receiving element is moved along the surface in the counter clockwise direction. Its final position is indicated by a ring in Figure 12. The same type of rectangular waveguide-fed aperture is used as in the experimental antenna, but the frequency is changed to 5 GHz. Furthermore, only a single mode approximation is used here and two surface rays are included in the simulations, one in each direction around the elliptic cylinder. Figure 13 shows the isolated coupling vs. the shape of the elliptic surfaces. Due to space limitations only the amplitude is shown.

As expected, the decay of the isolated mutual coupling is reduced when the surface gets flat but increases again when passing through the sharpest part of the surface. The ripple at large separations is caused by the interference of the two waves traveling in opposite directions around the elliptic cylinder. In this example, the UTD-MoM solution is once again pushed to its limit for some of the surfaces with very sharp edges. In the results shown here the local radii of curvature at the sharpest point are (starting with the circular cylinder) $r = 5\lambda$, 3.47λ, 1.25λ, and 0.14λ. And, as seen, the results have a reasonable behavior. However, the accuracy cannot be ascertained since no reference results have been found. The most important conclusion is, however, that the UTD solution gives satisfactory

results for many surfaces that are interesting from a practical engineering point of view.

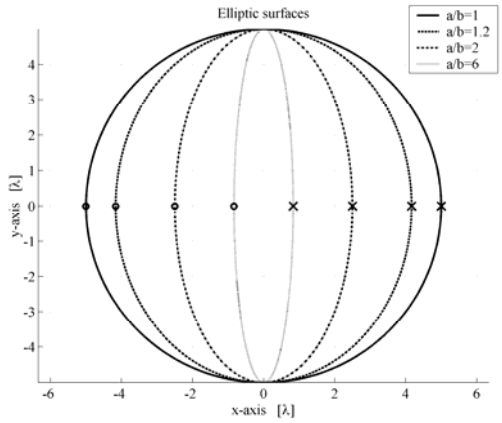

Figure 12. The different elliptic cylinders considered. A cross indicates the fixed position of the transmitting aperture, and a circle shows the final position of the second aperture. The circular cylinder is also shown for comparison.

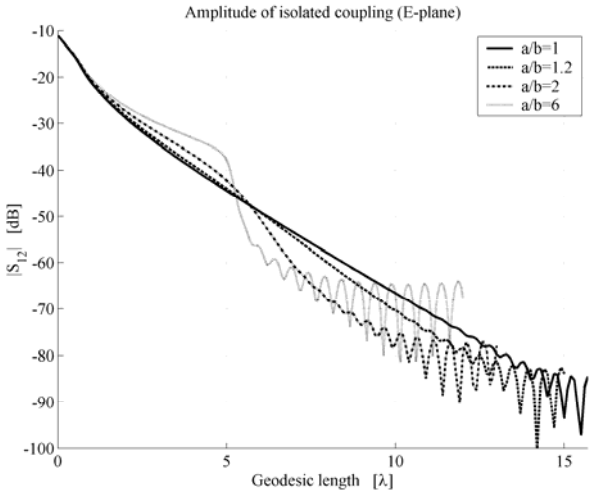

Figure 13. The amplitude of the isolated mutual coupling in the circumferential direction (*E* plane) for apertures at elliptic cylinders.

B. Doubly Curved Surfaces

The extension to doubly curved PEC surfaces is challenging and interesting. Unfortunately, the literature references in this area are not many and much remains to be investigated.

Shown here are some results for a doubly curved array, both mutual coupling results and radiation patterns are considered. The doubly curved experimental antenna

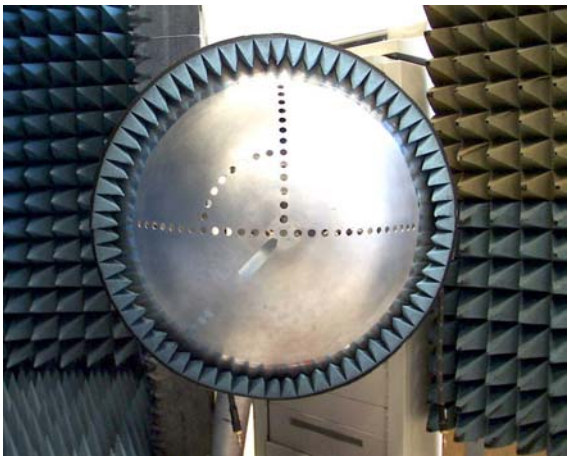

Figure 14. The geometry of the experimental doubly curved antenna. Courtesy of Ericsson Microwave Systems AB.

shown in Figure 14 was built at Ericsson Microwave Systems AB in Mölndal, Sweden, in 2000. The experimental antenna is shaped as a paraboloid of revolution with $f/d \approx 0.22$, and the diameter of the surface is approximately 600 mm with a depth of approximately 175 mm. Absorbers were placed on the edge to minimize edge effects. In this example circular waveguide-fed apertures are used, with a diameter of 14.40 mm. For practical reasons they are filled with Rexolite ($\varepsilon_r = 2.53$). The cutoff frequency for the dominant TE_{11}-mode is 7.65 GHz.

The surface has 48 circular apertures with the layout shown in Figure 14. The positions have been chosen to cover most element positions of interest in a doubly curved array, without covering the surface completely. In order to study polarization effects one of two orthogonal polarizations can be selected. This is achieved by rotating the waveguides by 90 degrees.

Figure 15 shows the isolated coupling along the principal plane of the paraboloid. The fed element is the element farthest away from vertex. Shown here is the *E*-plane coupling when using the dominant TE_{11}-mode only. Furthermore, only a single ray is accounted for in the simulations, but the first geodesic constant α is obtained with high accuracy (at least eight decimals). Measured results are also included here and the agreement is good. If the surface had been more pointed a slope change could have been observed when passing the vertex point $(s = 0\lambda)$.

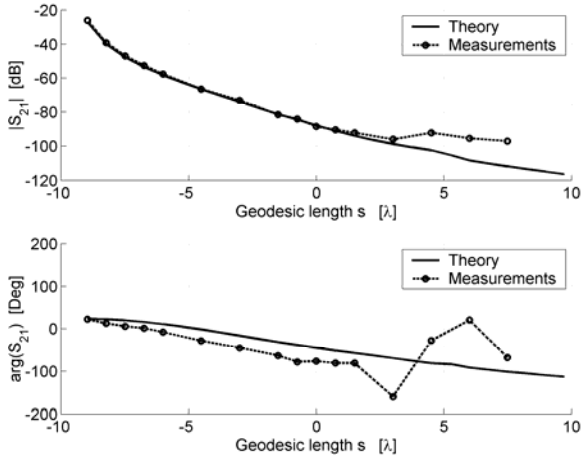

Figure 15. Isolated coupling along the principle direction of the paraboloid, *H* plane. Single mode approximation, $f = 8.975$ GHz.

The next example shows the isolated power pattern. If the element at vertex is element number 1, the pattern is shown for element number 7. Assume that the origin is at vertex and that the *z*-axis is pointing out of Figure 14, then the pattern is shown in a plane containing the symmetry axis of the paraboloid. The element is polarized in such a way that we get an *E*-plane pattern, and the result is shown in Figure 16 including measured data. Once again, only a single mode is used as well as a single ray. Note, however, that Kaifas et al. [26] shows that a ray caustic appears for certain element positions versus the shape of the surfaces. In these cases the single ray splits into three rays and has to be treated separately, but this does not appear for the cases considered here.

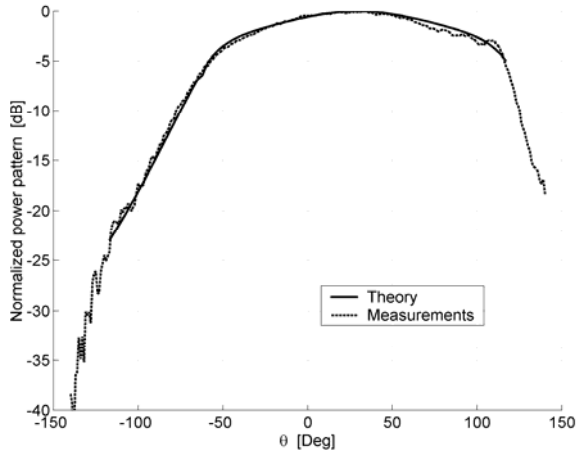

Figure 16. Calculated and measured power pattern (*E* plane) from a circular waveguide-fed aperture at the paraboloid. Single mode approximation, $f = 8.9$ GHz.

The results presented here are, to our knowledge, one of few where a UTD based method has been experimentally verified for a doubly curved surface. As seen, the agreement is good and it is possible to use UTD also for analyzing and designing doubly curved conformal array antennas.

Additional results (different polarization combinations, single element patterns, array patterns etcetera) can be found in [3, 27].

V. CONCLUSIONS

This paper presents an overview of the analysis of conformal array antennas. The focus is on the hybrid UTD-MoM method, and both singly and doubly curved PEC surfaces are considered. An important factor for accurate results is the problem of finding the geodesics. The reason is that it is possible to formulate the UTD-MoM solution in a single parameter form for certain types of surfaces. The solution then becomes directly related to the geodesics through the first geodesic constant α. Hence, the accuracy of the results depends exclusively on the accuracy of α. In this paper α is determined with an accuracy of at least eight decimal places.

The types of surfaces considered here belong to the geodesic coordinate system. This means that the parameter lines of the surface are orthogonal to each other, and any rotational symmetric doubly curved surface belongs to this class. For these cases the geodesics are found by quadrature, and in many cases the integral can be solved in closed form. This facilitates the analysis a lot.

As shown here, it is possible to generate very accurate results for different singly and doubly curved PEC surfaces by using the UTD-MoM approach. Both mutual coupling and radiation patterns have been considered. The results are verified by measured data obtained from two experimental antennas built at Ericsson Microwave Systems AB in Mölndal, Sweden. Furthermore, the limitation of the UTD formulation has been studied by comparing the results with results obtained from a modal solution. In conclusion, the hybrid UTD-MoM approach is surprisingly accurate both for electrically large and small PEC surfaces. Hence, the method is accurate enough to be used when designing conformal array antennas. However, more research is needed to be able to include coated surfaces. Some special cases can be handled, as indicated in this paper. But, there is today no verified tool for electrically large coated surfaces in general.

ACKNOWLEDGEMENT

Prof. Lars Josefsson at Chalmers University of Technology, Gothenburg, Sweden, is gratefully acknowledged for his valuable comments on this paper.

REFERENCES

[1] D. A. Wingert and B. M. Howard, "Potential Impact of Smart Electromagnetic Antennas on Aircraft Performace and Design," *NATO Workshop on Smart electromagnetic Antenna Structures*, Brussels, pp. 1.1-1.10, November 1996.

[2] Website: http://www.stealthsite.com/index.htm, 2005-09-13.

[3] L. Josefsson and P. Persson, *Conformal Array Antenna Theory and Design*, Wiley-IEEE Press, February 2006.

[4] J. R. Wait, *Electromagnetic Radiation from Cylindrical Structures*, Pergamon Press, 1959.

[5] R. F. Harrington, *Time Harmonic Electromagnetic Fields*, Prentice-Hall, 1961.

[6] J. J. H. Wang, *Generalized Moment Methods in Electromagnetics*, John Wiley & Sons, 1991.

[7] J. Jin, *The Finite Element Method in Electromagnetics*, John Wiley & Sons, 1993.

[8] D. A. McNamara, C. W. I. Pistorius, and J. A. G. Malherbe, *Introduction to The Uniform Geometrical Theory of Diffraction*, Artech House, 1990.

[9] P. H. Pathak, W. D. Burnside, and R. J. Marhefka, "A Uniform GTD Analysis of the Diffraction of Electromagnetic Waves by a Smooth Convex Surface," *IEEE Trans. on Antennas and Propagation*, Vol. AP-28, No. 5, pp. 631-642, September 1980.

[10] P. H. Pathak, N. Wang, W. D. Burnside, and R. G. Kouyoumjian, "A Uniform GTD Solution for the Radiation from Sources on a Convex Surface," *IEEE Trans. on Antennas and Propagation*, Vol. AP-29, No. 4, pp. 609-622, July 1981.

[11] P. H. Pathak and N. Wang, "Ray analysis of Mutual Coupling Between Antennas on a Convex Surface," *IEEE Trans. on Antennas and Propagation*, Vol. AP-29, No. 6, pp. 911-922, November 1981.

[12] P. Persson and R. G. Rojas, "High-frequency Approximation for Mutual Coupling Calculations Between Apertures on a Perfect Electric Conductor Circular Cylinder Covered with a Dielectric Layer: Nonparaxial Region," *Radio Science*, Vol. 38, No. 4, 2003.

[13] B. Thors and R. G. Rojas, "Uniform Asymptotic Solution for the Radiation from a Magnetic Source on a Large Dielectric Coated Circular Cylinder: Non-paraxial Region," *Radio Science*, Vol. 38, No. 5, 2003.

[14] Z. Sipus, P.-S. Kildal, R. Leijon, and M. Johansson, "An Algorithm for Calculating Green's Function of Planar, Cylindrical and Spherical Multilayer Substrates," *ACES Journal*, Vol. 13, No.3, pp. 243-254, Nov. 1998.

[15] C. A. Macon, L. C. Kempel, and S. W. Schneider, "Modeling Cavity-Backed Apertures Conformal to Prolate Spheroids Using the Finite Element-Boundary Integral Technique," *IEEE AP-S Intern. Symp.*, pp. 550-553, 2002.

[16] J. Boersma and S. W. Lee, "Surface Field due to a Magnetic Dipole on a Cylinder: Asymptotic Expansion of Exact Solution," Electromagnetics Laboratory, Technical Report No. 78-17, University of Illinois, December 1978.

[17] E. K. Yung, S. W. Lee, and R. Mittra, "GTD Solution of the Input Admittance of a Slot on a Cone," *IEEE AP-S. Intern. Symp.*, Vol. 17, pp. 667-670, 1979.

[18] T. S. Bird, "Accurate Asymptotic Solution for the Surface Field due to Apertures in a Conducting Cylinder," *IEEE Trans. on Antennas and Propagation*, Vol. AP-33, pp. 1108-1117, October 1985.

[19] G.-X. Fan and J. M. Jin, "Scattering from a Cylindrically Conformal Slotted Wavegudie Array Antenna," *IEEE Trans. on Antennas and Propagation*, Vol. 45, pp. 1150-1159, July 1997.

[20] D. J. Struik, *Lectures on Classical Differential Geometry*, Second edit., Dover Publications, Inc., 1988.

[21] R. M. Jha, S. A. Bokhari, V. Sudhakar, and P. R. Mahapatra, "Closed Form Surface Ray Tracing on Ogival Surfaces," *1989 IEEE AP-S Intern. Symp*., pp. 1294-1297, June 26-30, 1989.

[22] R. M. Jha and W. Wiesbeck, "The Geodesic Constant Method: A Novel Approach to Analytical Surface-Ray Tracing on Convex Conducting Bodies," *IEEE Antennas and Propagation Magazine*, Vol. 37, No. 2, pp. 28-38, April 1995.

[23] R. M. Jha, S. A. Bokhari, V. Sudhakar, and P. R. Mahapatra, "Geodesic Splitting on General Paraboloid of Revolution and its Implications to the Surface Ray Analysis," *1989 IEEE AP-S Intern. Symp*., pp. 223-226, June 26-30, 1989.

[24] R. C. Hansen, *Phased Array Antennas*, John Wiley & Sons, 1998.

[25] P. Persson and L. Josefsson, "Calculating The Mutual Coupling Between Apertures on a Convex Circular Cylinder Using a Hybrid UTD-MoM Method," *IEEE Trans. on Antennas and*

Propagation, Vol. AP-49, No. 4, pp. 672-677, April 2001.

[26] T. N. Kaifas, T. Samaras, K. Siakavara, and J. N. Sahalos, "A UTD-OM Technique to Design Slot Arrays on a Perfectly Conducting Paraboloid," *IEEE Trans. on Antennas and Propagation*, Vol. 53, No. 5, pp. 1688-1698, May 2005.

[27] P. Persson, L. Josefsson, and M. Lanne, "Investigation of the Mutual Coupling between Apertures on Doubly Curved Convex Surfaces: Theory and Measurements," *IEEE Trans. on Antennas and Propagation*, Vol. AP-51, No. 4, pp. 682-692, April 2003.

Patrik Persson was born in Stockholm, Sweden, in 1973. He received the M.Sc. Eng. and Ph.D. degrees in electromagnetic theory from the Royal Institute of Technology, Stockholm, in 1997 and 2002, respectively. He is currently employed as a research associate in the division of Electromagnetic Engineering, Royal Institute of Technology. His main research interests include conformal antennas, high-frequency techniques, and broad-band array antennas. Dr. Persson is the author of more than 40 journals and conference publications. He is also the coauthor of the book Conformal Array Antenna Theory & Design, published by Wiley-IEEE Press.

He spent 6 months of the academic year 2000-2001 at the ElectroScience Laboratory, Ohio State University, Columbus, Ohio as a visiting scholar, working on the development of high-frequency models for conformal antennas. He has also been a visiting scientist (part time, Feb. 2002-Apr. 2004) at the department of Physics and Measurements Technology, Division of Theoretical Physics, Linköping University in Sweden. During this period, he was involved with work on faceted conformal antennas. Patrik Persson has been involved in the organization of several European Workshops on Conformal Antennas (EWCA).

Dr. Persson received the 2002 R. W. P. King Prize Paper Award given by IEEE.